ACS SyntheticBiology

Letter

pubs.acs.org/synthbio

Rational Design of a Fusion Protein to Exhibit Disulfide-Mediated Logic Gate Behavior

Jay H. Choi and Marc Ostermeier*

Department of Chemical & Biomolecular Engineering, Johns Hopkins University, 3400 North Charles Street, Baltimore, Maryland 21218, United States

Supporting Information

ABSTRACT: Synthetic cellular logic gates are primarily built from gene circuits owing to their inherent modularity. Single proteins can also possess logic gate functions and offer the potential to be simpler, quicker, and less dependent on cellular resources than gene circuits. However, the design of protein logic gates that are modular and integrate with other cellular components is a considerable challenge. As a step toward addressing this challenge, we describe the design, construction, and characterization of AND, ORN, and YES logic gates built by introducing disulfide bonds into RG13, a fusion of maltose binding protein and TEM-1 β-lactamase for which maltose is an allosteric activator of enzyme activity. We rationally designed these disulfide bonds to manipulate RG13's allosteric regulation mechanism such that the gating had maltose and reducing agents as input signals, and the gates could be toggled between different gating functions using redox agents, although some gates performed suboptimally.

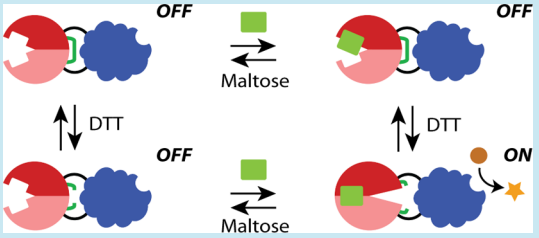

KEYWORDS: *logic gate, protein logic gate, allostery, disulfide bond, protein engineering, protein switch*

A central goal of synthetic biology is to build programmed cells that respond to exogenous or endogenous signals with a desired behavior. Two-input logic gates are a fundamental unit of decision-making and thus have been a focal point for building desired cellular function from the ground up. With a few notable exceptions,[1] the predominant focus has been on building transcriptional networks that function as logic gates, which are then combined to build more complex behavior.[2] The focus on transcriptional networks is well placed due to their inherently modular nature. However, the capacity of proteins as computational elements has long been appreciated.[3] Theoretically, proteins have the capacity to perform all 16 possible two-input logic gate operations.[4] Proteins as single-molecule level computational units offer a number of desirable attributes. Protein encoded logic operations do not rely on other cellular components for functionality, aside from the fact that they require cell components for their synthesis. A one molecule functional unit is inherently attractive for simplicity. Protein-based logic operations do not rely on transcription, translation, and protein degradation for functionality. Thus, computational operations can be performed more quickly and without the consumption of cellular resources. As a result, networks of proteins can be envisioned that perform complex operations inside or outside the cell. However, the complexity of proteins and generally their relative lack of modularity (compared to gene networks) are serious impediments to the realization of proteins' potential as logic gates that rival transcriptional networks.

One approach to building protein logic gates is to adapt natural allosteric proteins with gating behavior. For example, Lim and co-workers redesigned the modular allosteric protein N-WASP (which naturally functions as an AND gate) to function as AND and OR gates for new inputs.[5] Here, we explore the adaptability of engineered allosteric enzymes to exhibit different logic gate functions. We have previously constructed β-lactamase enzymes that are positively regulated by maltodextrins by inserting circular permutations of TEM-1 β-lactamase into the *E. coli* maltose binding protein (MBP).[6,7] MBP undergoes a large conformational change that consists of a hinge bending motion such that the two domains of MBP close upon the maltodextrin.[8] A variety of biochemical and biophysical studies indicate that at least one of our protein switches, RG13, functions by an allosteric mechanism dependent on this conformational change in the MBP domain.[6,9,10] We designed our protein switches to function as a simple, single input YES gate for maltose. We confirmed this property both *in vitro* (by enzymatic assay) and *in vivo* (by measuring the β-lactam resistance of cells expressing the switches in the absence and presence of maltose).[6,7] Although we designed these switches with only YES gate functionality in mind, we have shown that the switches also possessed OR and ANDN gate functionality. This gating behavior was predicable from the biochemical and structural properties of MBP. As both maltose and maltotriose induce similar conformational changes in MBP, both maltose and maltotriose activate RG13,[6] constituting OR gate behavior. As β-cyclodextrin (a large cyclic maltodextrin) binds to the same site in MBP as maltose but induces only a small change in conformation,[11] it is not too surprising that RG13 is an ANDN gate for maltose and β-cyclodextrin, since β-

Received: May 21, 2014
Published: August 21, 2014

   dx.doi.org/10.1021/sb500254g | *ACS Synth. Biol.* 2015, 4, 400−406

cyclodextrin, at sufficient concentrations, prevents activation by maltose.[6] Finally, we have also redesigned a related switch, MBP317-347, to function as an OR gate for sucrose and maltose by introducing mutations into the binding site of the MPB domain that conferred sucrose binding without eliminating maltose binding.[7]

Here, we further tested the ability of RG13 to be engineered to function as logic gates. We used a rational design approach involving engineered disulfides to redesign RG13 to function as AND, ORN, and YES gates for new inputs. We were inspired by the fact that cellular responses to oxidative conditions often involve redox-controlled proteins with cysteines that can be reversibly oxidized. Disulfide bond formation between the cysteines can serve as redox-sensing mechanism that detects cellular oxidizing factors such as oxygen, reactive oxygen species, and cellular reducing factors such as thioredoxin, and glutathione.[12] Disulfide formation/reduction can modulate the protein function directly via affecting functional residues or indirectly via conformational changes.[12,13] Accordingly, many researchers have successfully engineered redox control over protein function through the introduction of cysteines at the proper position in the protein structure such that disulfide bond formation/reduction mediates protein structure and function.[14,15] Here, we integrated redox-control into RG13 by introducing disulfide bonds to keep the MBP domain in either an open or closed conformation in order to elicit AND, ORN, and YES gate behavior. Although some gates behaved suboptimally, we show that the maltose-regulated allostery of RG13 can be rendered dependent on whether the disulfide bond is present or not; hence, the effector-controlled switching property can be turned on or off by redox agents. Our results illustrate one way in which protein switches can be rationally redesigned to execute different logic gate functions through a manipulation of their allosteric mechanism.

RESULTS AND DISCUSSION

Rationale for the Design of New Gating Behavior into Protein Switch RG13. RG13 consists of a circularly permutation of BLA inserted in place of residue 317 of MBP. In the absence of maltose, the enzymatic activity of RG13 is compromised relative to BLA (k_{cat}/K_m of RG13 is about 4% of the value of BLA), but maltose binding restores activity to a level equivalent to that of BLA.[6] In addition, the gene encoding RG13 confers a switching phenotype to *E. coli* cells as maltose increases the ampicillin resistance over the resistance observed in the absence of maltose.[6] MBP is known to undergo a hinge-bending conformational change from an open to a closed state upon binding maltose.[8] A variety of biochemical and biophysical evidence indicates that a very similar conformational change occurs in RG13 and that this conformational change is responsible for switching. First, mutations in the hinge region of MBP that are known[16] or suspected to cause partially closed states in MBP decrease the magnitude of switching (ratio of enzymatic activity in the presence of maltose to that in the absence of maltose) by raising the activity in the absence of maltose.[6,10] Second, the fluorescence[6] and NMR[9] spectra of RG13 in the absence and presence of maltose is consistent with the MBP domain of RG13 being in the open and closed state, respectively.

Based on these studies, we hypothesized that the switching behavior of RG13 could be altered by manipulating the state of the MBP domain with engineered disulfide bonds (Figure 1). An important criterion in our design was to place the disulfide

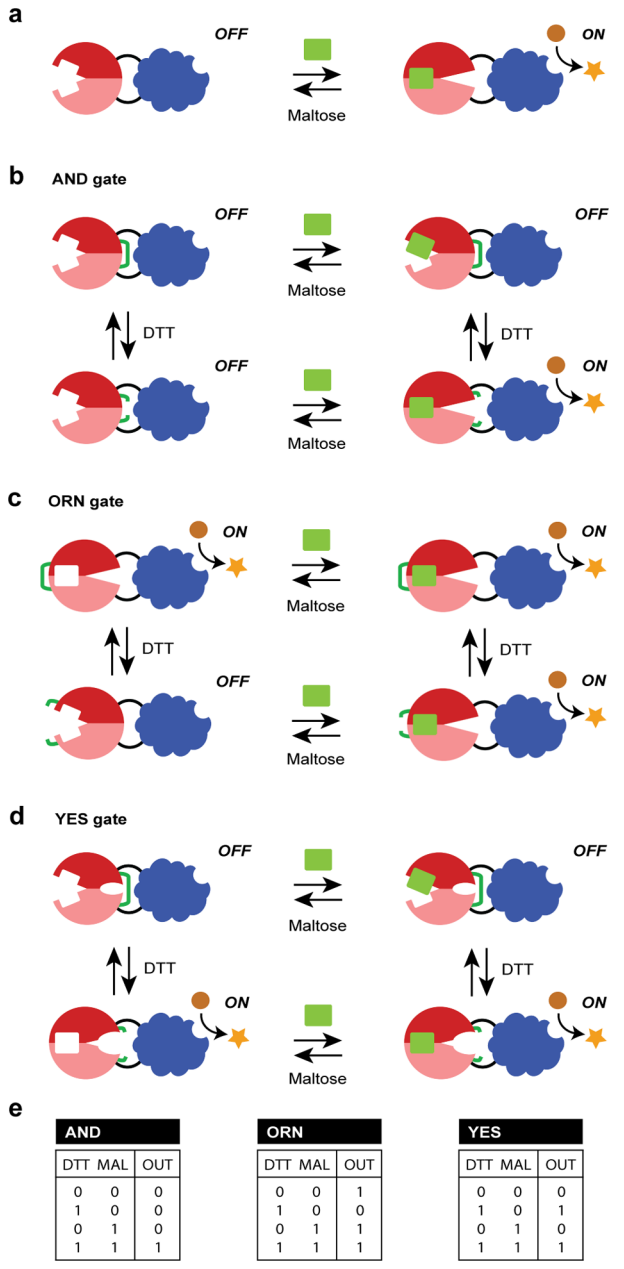

Figure 1. Idealized logic gate design. (A) The switching mechanism of RG13, a protein comprised of a BLA domain (blue) and MBP domain, whose two subdomains are colored in red and pink. RG13's ability to convert β-lactam antibiotics (circle) into an inactive form (star) is dependent on maltose (green square) and the conformational change in the MBP domain upon binding maltose. Note that the enzymatic activity of RG13 is not completely off in the absence of maltose, and the designation of the state as "off" is meant to convey a less active state. RG13 is a YES gate for maltose. (B) AND gate design. A disulfide bond (green line) introduced in the hinge region holds the MBP domain in an open conformation. Activation of enzyme activity requires both maltose and reduction of the disulfide bond with DTT. (C) ORN gate design. A disulfide bond (green line) is introduced to hold the MBP domain in the closed state resulting in an active enzyme domain. The switch is in an off state only if the disulfide is reduced with DTT and maltose is absent. (D) Inversion of RG13 YES gate behavior. In addition to a disulfide in the hinge region holding the MBP domain in the open conformation, mutations in the hinge destabilize the open conformation such that reduction with DTT is sufficient to activate enzyme activity. (E) The truth tables that describe the three logic gates.

dx.doi.org/10.1021/sb500254g | ACS Synth. Biol. 2015, 4, 400−406

bonds away from the effector binding and enzymatic active sites so as to not directly perturb their properties. We sought to achieve redox control over the conformational equilibria between the closed and open state of the MBP domain. We reasoned that the proper placement of a disulfide bond in the hinge region could hold the MBP domain in the open conformation regardless of the presence of maltose, resulting in AND gate behavior for maltose and a reducing agent (Figure 1B). Conversely, a disulfide placed to hold the MBP domain in a closed position even in the absence of maltose would result in ORN gate behavior, with enzymatic activity being in an off state only in the presence of reducing agents and the absence of maltose (Figure 1C). Finally, a disulfide in the hinge region combined with mutations that selectively weaken the stability of the open conformation (for example by disrupting interactions in the hinge region) would convert RG13 from a YES gate for maltose to one that was a YES gate for a reducing agent (Figure 1D). This particular case would be an example of converting an effector-controlled protein switch to redox-mediated protein switch.

The use of a reducing agent as an input for the gates results in gating behavior that is dependent on the state of the disulfide bond, and thus, our proposed gates have the added complexity of a toggle switch function. For example, a hypothetical AND gate (in the state with a disulfide bond) that requires maltose and a reducing agent for activation does not require the reducing agent for activation once the disulfide is not present. In this context, the redox agent can be thought of as an input that toggles the protein from being an AND gate for maltose and reducing agent to an ANDN gate for oxidizing agent and maltose. Likewise, for our proposed ORN gate, the redox agent toggles the protein from being an ORN gate for reducing agent and maltose to an OR gate for oxidizing agent and maltose.

Identification of the Locations for the Engineered Disulfide Bonds in RG13. We utilized the only available crystal structure of RG13 (PDB ID: 4DXC),[17] which was obtained in the presence of Zn^{2+} and the absence of maltose, recognizing the limitation that Zn^{2+} is a negative effector that noncompetitively switches off enzyme activity. We sequentially replaced all possible pairs of residues in RG13 with cysteines and predicted the disulfides based on their geometrical constraints using the side-chain conformation prediction algorithm, SCWRL.[18] Of the 202 566 possible pairs of residues, 11 pairs were identified as possible target locations for cysteine substitution. We further reduced this to four pairs by requiring that one residue should be located in each of the subdomains of the MBP domain of RG13.

We built models of these four RG13 variants. The cysteines of RG13-AND1 (A301C/M588C) and RG13-AND2 (E308C/G584C) are located in the hinge region on the opposite side of the protein from the maltose-binding site (Figure 2B). Residues 301 and 308 reside on the N-terminal domain, and residues 588 and 584 reside on the C-terminal domain. We predicted the length of disulfide bonds in RG13-AND1 and RG13-AND2 to be 2.08 and 1.88 Å, respectively. Disulfide bond formations in both constructs were expected to lock the MBP domain in the open conformation and elicit AND gate behavior as per Figure 1B. The cysteines of RG13-ORN1 (P229C/P298C) and RG13-ORN2 (Q72C/P601C) are located on the side of MBP at which maltose binds (Figure 2C). Residues 298 and 72 reside on the N-terminal domain and residues 229 and 601 reside on the C-terminal domain. We predicted the length of disulfide bonds in RG13-ORN1 and RG13-ORN2 to be 2.02 and 2.37 Å,

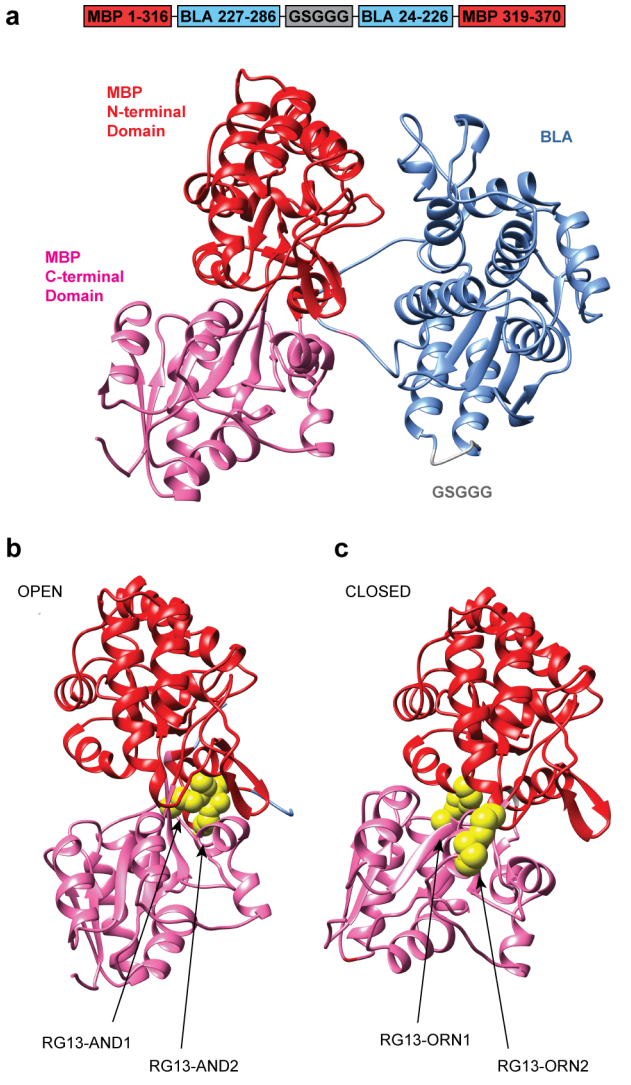

Figure 2. Sequence and structure RG13 (PDB ID: 4DXC) with engineered disulfide bonds. (A) A graphical illustration of the RG13 sequence based on the MBP and BLA domain. The MBP domain sequences are in red, BLA domain sequence is in blue, and the linker region is shown in gray. In the MBP domain in the ribbon diagram, the N-terminal domain (residue 1−110 and 261−316) is in pink and the C-terminal domain (residue 111−260 and 585−637) is in red. (B) The open conformation of the MBP domain (PDB ID: 1OMP) with engineered disulfide bonds for RG13-AND1 (A301C + M588C) and RG13-AND2 (E308C + G584C) shown in yellow spheres. (C) The closed conformation of the MBP domain (PDB ID: 1ANF) with engineered disulfide bonds for RG13-ORN1 (P229C + P298C) and RG13-ORN2 (Q72C + P601C) shown in yellow spheres.

respectively. We predicted that disulfide bond formation in these two would lock the two subdomains of the MBP domain in the closed conformation and elicit ORN gate behavior, as depicted in Figure 1C.

Switching Cellular Phenotype Shows Redox-Dependent, Maltose-Controlled Switching Behavior. We constructed the set of four mutants RG13-AND1, RG13-AND2, RG13-ORN1, and RG13-ORN2 on the platform of RG13-AA, a variant of RG13 in which the two cysteines native to the BLA domain that normally participate in a disulfide bond were mutated to alanine (Table 1 and Supporting Information Figure 1). We removed these cysteines to prevent improper intramolecular disulfide formation and eliminate the possibility

dx.doi.org/10.1021/sb500254g | ACS Synth. Biol. 2015, 4, 400−406

Table 1. Primary Sequence and List of Mutations of the Proteins Used in This Study

protein	protein sequence[a]/mutations
RG13	MBP[1−316]-BLA[227−286]-GSGGG-BLA[24−226]-S-MBP[319−397]-6xHis
RG13-AA	RG13 C433A + C479A
RG13-AND1	RG13 C433A + C479A + A301C + M588C
RG13-AND2	RG13 C433A + C479A + E308C + G584C
RG13-YES	RG13 C433A + C479A + E308C + G584C + M588A + Q592A
RG13-ORN1	RG13 C433A + C479A + P229C + P298C
RG13-ORN2	RG13 C433A + C479A + Q72C + P601C

[a]Based on gene sequencing. A sequence alignment can be found in Supporting Information Figure 1.

that any affect observed depended on the state of this native disulfide in the BLA domain. The removal of this disulfide bond of the BLA domain has no effect on the switching activity of RG13.[19] We initially assessed the gating behavior of these constructs by the ampicillin resistance phenotype their genes confer to *E. coli*. We measured the ratio of the minimum inhibitory concentration of ampicillin (MIC_{Amp}) in the presence and absence of maltose and the reduced form of glutathione (GSH) in the growth media.

The maltose-dependent MIC_{Amp} ratio of RG13-AA remained unchanged in 0 mM and 3 mM GSH, suggesting that GSH has no inherent effect on the enzymatic activity of the BLA domain (Figure 3A) and that the switching activity is unaffected by the change in redox potential. Of the four design constructs, RG13-AND1 and RG13-ORN1 did not show a significant maltose effect on Amp resistance under any conditions and were not investigated further (Supporting Information Table 1). In contrast, the gene encoding RG13-AND2 conferred an AND gate phenotype to *E. coli*. GSH was required for maltose to cause an 8-fold increase in the MIC_{Amp} (Figure 3B). This supports the hypothesis that the engineered disulfide bond in RG13-AND2 would keep the MBP domain in an open conformation until the disulfide is reduced. Once the disulfide bond is reduced, maltose-regulated allostery and subsequent switching behavior are shown in maltose-dependent ampicillin resistance. This result also provides additional evidence that maltose-dependent closing of the MBP domain causes the increase in enzyme activity for RG13.

Although RG13-ORN2 did not confer ORN gate behavior to *E. coli* as designed, the MIC_{Amp} increased significantly in the presence of maltose, both in the absence and presence of GSH (Figure 3C). RG13-ORN2 did not confer ORN gate behavior because the MIC_{Amp} was not high in the absence of both maltose and GSH. However, interpretation of switching phenotypes is complicated by the fact that a maltose-dependent switching phenotype results from one or both of two mechanisms:[20,21] (1) maltose-binding increases the specific catalytic activity of the switch, and (2) maltose increases the cellular abundance of the switch, resulting in an increase in ampicillin hydrolysis activity in the cell. A disulfide bond holding the MBP domain in the closed conformation might compromise the abundance of the switch unless maltose is present to stabilize the protein. In addition, the observation of the desired switching types depends to some extent on our ability to maintain the desired reduced or oxidized state in the periplasm throughout the culturing of the cells. Potentially the cell's inherent mechanisms for controlling the oxidizing conditions of the periplasm, the cellular compartment in which the switches are expressed, could complicate our experiments. For these reasons we decided to investigate the gating behaviors of RG13-AND2 and RG13-ORN2 *in vitro*.

RG13-AND2 and RG13-ORN2 Exhibit Gating Behavior *In Vitro*. We purified RG13-AA, RG13-AND2, and RG13-ORN2 and measured their enzymatic activity in the presence and absence of maltose with and without the reducing agent DTT. All three proteins purified as a single species of the same size in size exclusion chromatography and had a free thiol content of <1% as measured using Ellman's reagent. These results indicate that the cysteines in RG13-AND2 and RG13-ORN2 were in an intramolecular disulfide bond as designed. In the absence of maltose, RG13-AA enzyme activity remained approximately the same both in the presence and absence of DTT without maltose presence, indicating that DTT did not inherently alter the enzymatic activity of the BLA domain (Figure 3A). As expected, the addition of maltose, increased enzymatic activity of RG13-AA regardless of the presence of DTT. In contrast, RG13-AND2 was significantly compromised in maltose activation in the absence of DTT, although some maltose activation was apparent (Figure 3B). Similarly, DTT had some ability by itself to activate enzymatic activity. However, enzyme activity in the presence of both maltose and DTT was 41% higher than would be predicted by the additive effects of maltose and DTT individually. Additionally, the levels of enzyme activity in the presence of both maltose and DTT were the same for RG13-AND2 and RG13-AA, indicating that only in the presence of both compounds is the enzymatic activity of RG13-AND2 fully activated. Thus, RG13-AND2 is controlled by two input signals (ligand binding and change in redox potential) and exhibits AND gate behavior. The maltose-dependent allosteric mechanism of RG13-AND2 cannot be fully activated until the engineered disulfide bond is reduced by changing the redox potential.

The enzymatic activity of RG13-ORN2 had the fundamental property of an ORN gate: activity was lowest when one but not both of the two inputs was present (Figure 3C). In the absence of maltose, RG13-ORN2 showed a 54% decrease in enzyme activity with addition of DTT. This result is qualitatively consistent with the expected role of the disulfide on enzyme activity, keeping the MBP domain in a closed conformation such that the BLA domain is more active even in the absence of maltose. However, the disulfide bond alone does not fully activate the switch, perhaps because the disulfide causes a closed conformation that is not equivalent to the one caused by maltose and one that does not fully activating the enzyme domain. The ability of maltose to further activate the disulfide bond form of RG13-ORN2 is consistent with this view.

RG13-YES: Inverting a YES Gate. Although RG13-AND2 exhibited AND gate behavior, it was partially activated by the addition of DTT alone (Figure 2B). One potential reason is that the E308C/G584C mutations partially destabilize the hinge region that helps keep the MBP domain in the open conformation. In the absence of the disulfide (i.e., with the addition of GSH), this destabilization shifts the MBP open/closed equilibrium more toward the closed conformation, resulting in the observed increase in enzyme activity. This hypothesis inspired us to attempt to invert the YES gate functionality of RG13-AA, by introducing mutations into RG13-AND2 designed to further destabilize the hinge such that the enzyme activity could be controlled with only the redox potential independent of maltose binding. Alanine mutations in MBP at the equivalent residues Met588 and

dx.doi.org/10.1021/sb500254g | *ACS Synth. Biol.* 2015, 4, 400−406

a RG13-AA

	RED	MAL	OUT	MIC (μg/mL)	Initial Rate (sec^{-1})
	0	0	0	64	46 ± 3
	1	0	0	64	42 ± 16
	0	1	1	512	466 ± 152
	1	1	1	512	484 ± 70

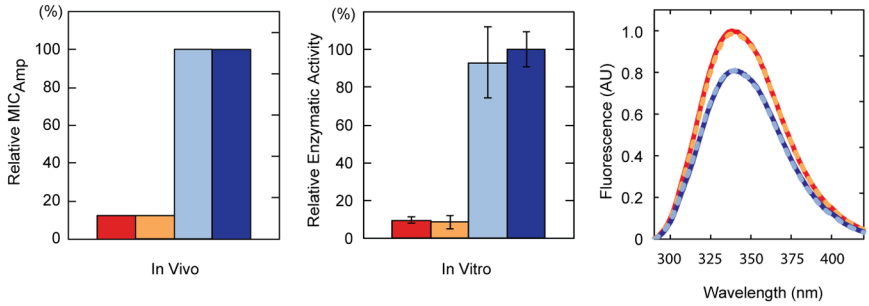

b RG13-AND2

	RED	MAL	OUT	MIC (μg/mL)	Initial Rate (sec^{-1})
	0	0	0	64	27 ± 7
	1	0	0	64	187 ± 26
	0	1	0	64	113 ± 11
	1	1	1	256	483 ± 30

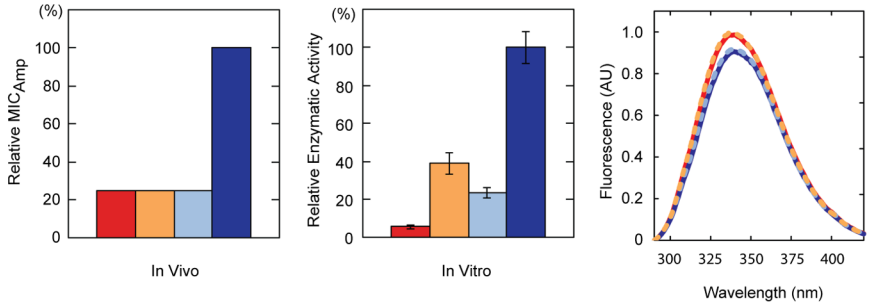

c RG13-ORN2

	RED	MAL	OUT	MIC (μg/mL)	Initial Rate (sec^{-1})
	0	0	1	64	232 ± 18
	1	0	0	64	108 ± 27
	0	1	1	512	496 ± 67
	1	1	1	1024	564 ± 19

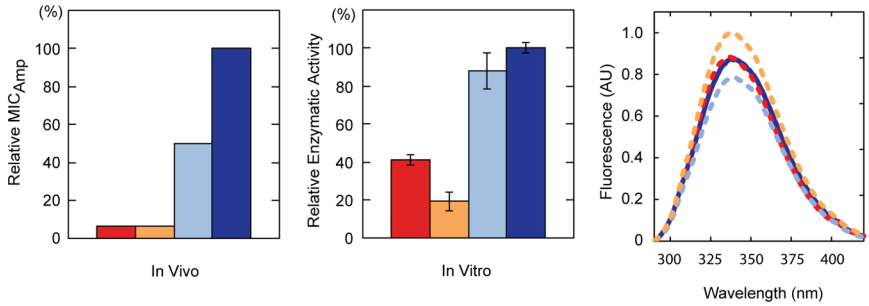

d RG13-YES

	RED	MAL	OUT	MIC (μg/mL)	Initial Rate (sec^{-1})
	0	0	0	32	52 ± 17
	1	0	1	128	400 ± 25
	0	1	0	64	114 ± 45
	1	1	1	512	497 ± 54

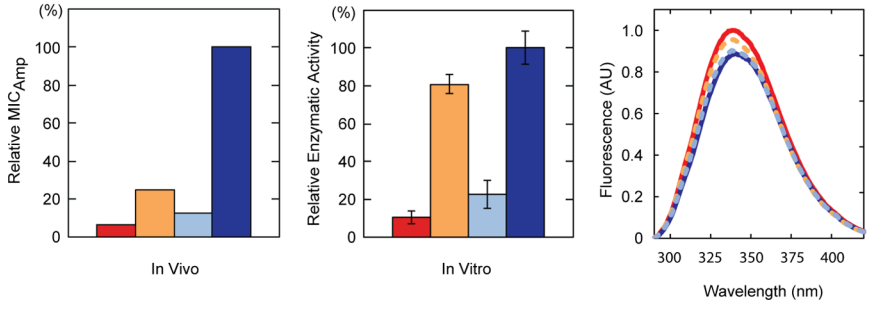

Figure 3. Logic gate performance and fluorescence characterization for (A) RG13-AA, (B) RG13-AND2, (C) RG13-ORN2, and (D) RG13-YES. For each of the designs in Figure 1, the gating behavior in cells (left bar graph) and *in vitro* (right bar graph) is presented for the inputs of reducing agent (red.) and maltose. The numerical values for these two graphs are presented in the table along with the respective truth table and color key. Cellular gating was measured by the minimum inhibitory concentration for ampicillin (MIC_{Amp}). The values presented are the median of three trials (data for all trials in Supporting Information Table 1). *In vitro* gating was measured by enzymatic activity for nitrocefin hydrolysis using purified protein. The values presented are the mean of three independent trials and the standard deviation. The fluorescence spectra under the four input conditions are presented on the right. The reducing agents used were GSH (cells), DTT (enzyme assays), and TCEP (fluorescence). Red, neither reducing agent nor maltose; orange, presence of reducing agent; light blue, presence of maltose; dark blue, presence of reducing agent and maltose.

Gln592 in RG13 greatly increased the maltose binding affinity.[22] These mutations did not cause significant structural changes in either the closed or open conformation of MBP, but rather removed interactions in the hinge that shifted the equilibrium of conformational states toward the closed conformation such that the binding affinity could be greatly increased.[22] Inspired by this study, we introduced the M588A and Q592A mutations into RG13-AND2 to create RG13-YES. Although the results *in vivo* were promising, RG13-YES most clearly exhibited the desired DTT YES gate behavior *in vitro* (Figure 3D). RG13-YES retained RG13-AND2's inability to be activated by maltose in the absence of DTT, but now could be almost fully activated by DTT alone. RG13-YES represents a

dx.doi.org/10.1021/sb500254g | *ACS Synth. Biol.* 2015, 4, 400−406

nearly complete inversion of the YES gate functionality of RG13-AA for maltose to a YES gate functionality for DTT.

Conformational Changes As Monitored by Intrinsic Protein Fluorescence. We next interrogated conformational changes in the switches using intrinsic protein fluorescence. MBP exhibits a quenching of fluorescence and small shift in the maximum fluorescence wavelength upon maltose binding owing to the presence of several tryptophans in the vicinity of the maltose-binding pocket,[11] a behavior that RG13 shares.[6] Since DTT quenches the fluorescence signal, TCEP was used as an alternative reducing agent. We confirmed that TCEP and DTT had equivalent effects on the enzymatic activity of RG13-AND2 (data not shown).

For all variants, maltose caused a decrease of fluorescence intensity and a slight shift of the emission spectrum within the range of 345−350 nm with or without TCEP. We interpret this result as indicating that all constructs bind maltose. For RG13-AA, maltose quenched the fluorescence and TCEP exhibited no effect on the fluorescence spectrum, as expected (Figure 3A). The maltose quenching of fluorescence of RG13-AND2 (Figure 3B) was TCEP independent as was RG13-AA but not as substantial as in RG13-AA. This spectroscopic result was inconsistent with the simplistic expectation that enzymatic activity should be inversely correlated to fluorescence quenching. However, maltose may still be able to bind in the presence of the disulfide, which results in a fluorescence change, but it may not activate enzyme activity due the engineered disulfide bond, which keeps the conformational equilibrium toward the open state. Alternatively, since BLA is inserted near the hinge region of MBP, the disulfide may interfere with the coupling of maltose-binding and enzyme activity. In contrast, the fluorescence behavior of RG13-ORN2 qualitatively matched the simplistic expectation. Unlike with RG13-AA and RG13-AND2, TCEP alone increased RG13-ORN2 fluorescence intensity, consistent with a conversion from a disulfide-forced closed conformation to the open conformation (Figure 3C). The introduction of the hinge-destabilizing E308C/G584C into RG13-AND2 to create RG13-YES caused a TCEP-dependent change in fluorescence in the absence of maltose to appear (Figure 3D). The effect of TCEP on RG13-YES in the absence of maltose was opposite of that on RG13-ORN2, causing a decrease in fluorescence (as expected for a change toward the closed state). However, similar to RG13-AA and RG13-AND2, RG13-YES showed no TCEP difference in the spectra in the presence of maltose despite the large difference in enzyme activity

Perspective. By modulating the conformational equilibrium of RG13's MBP domain with disulfide bonds without intentionally altering the molecular recognition of the input and output domains, we developed three switchable enzymes that could respond to a change in redox conditions. These proteins, which we built from the same starting protein switch, exhibited the three designed logic gate functions *in vitro*. In two out of three cases, the genes for these proteins conferred the same logic gate behavior to *E. coli* cells. Although we did not realize ideal logic gating behavior, our study demonstrates the potential for a single protein to be engineered to have multi-input control and different logic gate behavior. Although the integration of protein logic gates into genetic circuits will be challenging, we note that the protein logic gates described here, despite being a model system, should be able to be integrated into our previously design band-pass circuit in which gene expression was tied to β-lactam levels and the amount of cellular β-lactamase activity.[23] Finally, the use of redox conditions has potential practical applications, since cellular compartments can have different redox states. For example, an enzyme with AND gate behavior such as RG13-AND2 resulting in selective therapeutic properties can be envisioned that makes enzymatic prodrug activation depend on entry of the AND gate into the reducing environment of the cytosol and the presence of a cancer marker.[24]

METHODS

Materials. All chemicals used were purchased from Sigma (St. Louis, MO) unless otherwise noted. Nitrocefin was purchased from EMD Millipore (Billerica, MA). BL21 competent cells purchased from Agilent Technologies (Santa Clara, CA). pDIMC8-RG13, the plasmid that contain the RG13 gene, was previously described.[6,9] pDIMC8-RG13 was used as a template plasmid DNA to make variants using the PCR-based QuikChange mutagenesis procedure by Agilent Technologies. DNA of regions containing the targeted codon was sequenced and confirmed by Genewiz (Germantown, MD).

Identifying Target Residues for Engineering Disulfide Bonds and Molecular Modeling of Disulfide Bonds-Engineered RG13 Variants. All possible pairs of residues in the molecular structure of RG13 (PDB ID: 4DXC) were systematically substituted with cysteines, and disulfide bonds were predicted using SCWRL 4.1.[18] Once the target residues for engineering disulfide bonds were identified, the molecular models were constructed on the scaffold of RG13. The pairs of target residues were replaced with cysteines, and the side chain positions were subsequently optimized by using SCWRL 4.1. The final models were optimized by energy minimization using the GROMACS 4.1.3 package.[25] The models were visualized, and the disulfide bonds were examined using UCSF Chimera.[26]

MIC_{Amp} Assay. The liquid culture MIC_{Amp} assay was performed as previously described.[20,21] BL21 cells were transformed with pDIMC8 plasmids containing genes that encode the protein variants. For each overnight culture, 5 mL of tryptone broth (10 g/L tryptone and 10 g/L NaCl) was inoculated by picking a single colony and incubated in a 37 °C shaker for 16−18 h. The optical density at 600 nm ($OD_{600\ nm}$) of the cultures was measured. Approximately 1×10^6 colony forming unit (based on $OD_{600\ nm}$) from these cultures was added to 1 mL of tryptone medium containing chloramphenicol (*Cm*, 50 μg/mL), isopropyl-β-D-thiogalactopyranoside (IPTG, 300 μM), Amp (0 to 8192 μg/mL, in 2-fold increments), and either the absence or presence of 10 mM maltose and the absence or presence of 3 mM of GSH in each well of a 96-well assay block (Corning, Tewksbury, MA). Cultures were incubated in a shaker incubator at 25 °C for 28−32 h. An additional 5 mM GSH was added after 12 h of incubation. The MIC_{Amp} was defined as the lowest concentration of ampicillin at which the $OD_{600\ nm}$ was <5% of the $OD_{600\ nm}$ in the absence of ampicillin.

Expression and Purification of RG13 Variants. Proteins were expressed and purified from BL21 cells grown in M9 minimal media, as previously described.[21] Proteins were dialyzed against 5 L of a dialysis buffer (50 mM phosphate, pH 7.2). Approximately 5 mg of purified proteins were obtained with >95% purity, as estimated by coomassie blue staining of SDS-PAGE gels.

Nitrocefin Hydrolysis Enzymatic Assay. Enzymatic assays were performed as previously described[20,21] in 200 mM sodium phosphate buffer, pH 7.5 at a final protein

dx.doi.org/10.1021/sb500254g | ACS Synth. Biol. 2015, 4, 400−406

concentration of 1 to 5 nM. Proteins were incubated in the absence and presence of 10 mM maltose and the absence or presence of 2 mM of dithiothreitol (DTT) for 30 min at 25 °C. Nitrocefin was added to the final concentration of 50 μM. The absorbance at the wavelength of 486 nm was recorded by using a SpectraMax Plus^{384} Microplate Reader (Molecular Devices) and the initial rate of nitrocefin hydrolysis reaction was determined by SoftMax Pro 5.0 software package.

Intrinsic Protein Fluorescence. Proteins (0.3 μM) were incubated at 25 °C for 30 min in 200 mM sodium phosphate buffer (pH 7.5) containing 10 mM tris(2-carboxyethyl)-phosphine (TCEP), 10 mM maltose, 10 mM TCEP, and 10 mM maltose, or neither TCEP nor maltose before measuring the fluorescence. Fluorescence emission spectra were recorded in a PTI Quantamaster 30 Fluorescence Spectrofluorometer (Photon Technology International, Edison, NJ) with excitation at 280 nm and spectral bandwidths of 2 nm (excitation) and 4 nm (emission) using quartz cuvette (path length of 1.0 cm). All spectra were recorded at 25 °C and baseline-corrected.

■ ASSOCIATED CONTENT

Supporting Information

Supplemental Table 1 and Supplemental Figure 1 as described in the text. This material is available free of charge via the Internet at http://pubs.acs.org.

■ AUTHOR INFORMATION

Corresponding Author

*Email: oster@jhu.edu.

Notes

The authors declare the following competing financial interest(s): M.O. has issued and pending patents on protein switches.

■ ACKNOWLEDGMENTS

We thank Sarah Brown for preparing reagents and media. This work was supported by the Defence Threat Reduction Agency [HDTRA1-09-1-0016] and the National Institute of General Medicine at the National Institutes of Health [R01 GM066972].

■ REFERENCES

(1) Lim, W. A. (2010) Designing customized cell signalling circuits. *Nat. Rev. Mol. Cell Biol. 11*, 393−403.

(2) Khalil, A. S., and Collins, J. J. (2010) Synthetic biology: Applications come of age. *Nat. Rev. Genet. 11*, 367−379.

(3) Bray, D. (1995) Protein molecules as computational elements in living cells. *Nature 376*, 307−312.

(4) de Ronde, W., Rein ten Wolde, P., and Mugler, A. (2012) Protein logic: A statistical mechanical study of signal integration at the single-molecule level. *Biophys. J. 103*, 1097−1107.

(5) Dueber, J. E., Yeh, B. J., Chak, K., and Lim, W. A. (2003) Reprogramming control of an allosteric signaling switch through modular recombination. *Science 301*, 1904−1908.

(6) Guntas, G., Mitchell, S. F., and Ostermeier, M. (2004) A molecular switch created by *in vitro* recombination of nonhomologous genes. *Chem. Biol. 11*, 1483−1487.

(7) Guntas, G., Mansell, T. J., Kim, J. R., and Ostermeier, M. (2005) Directed evolution of protein switches and their application to the creation of ligand-binding proteins. *Proc. Natl. Acad. Sci. U.S.A. 102*, 11224−11229.

(8) Duan, X., Hall, J. A., Nikaido, H., and Quiocho, F. A. (2001) Crystal structures of the maltodextrin/maltose-binding protein complexed with reduced oligosaccharides: Flexibility of tertiary structure and ligand binding. *J. Mol. Biol. 306*, 1115−1126.

(9) Wright, C. M., Majumdar, A., Tolman, J. R., and Ostermeier, M. (2009) NMR characterization of an engineered domain fusion between maltose binding protein and TEM1 β-lactamase provides insight into its structure and allosteric mechanism. *Proteins 78*, 1423−1430.

(10) Kim, J. R., and Ostermeier, M. (2006) Modulation of effector affinity by hinge region mutations also modulates switching activity in an engineered allosteric TEM1 β-lactamase switch. *Arch. Biochem. Biophys. 446*, 44−51.

(11) Hall, J. A., Ganesan, A. K., Chen, J., and Nikaido, H. (1997) Two modes of ligand binding in maltose-binding protein of *Escherichia coli*. Functional significance in active transport. *J. Biol. Chem. 272*, 17615−17622.

(12) Nagahara, N. (2011) Intermolecular disulfide bond to modulate protein function as a redox-sensing switch. *Amino Acids 41*, 59−72.

(13) Ryu, S. E. (2012) Structural mechanism of disulphide bond-mediated redox switches. *J. Biochem. 151*, 579−588.

(14) Peng, Q., Kong, N., Wang, H. C., and Li, H. (2012) Designing redox potential-controlled protein switches based on mutually exclusive proteins. *Protein Sci. 21*, 1222−1230.

(15) Ostergaard, H., Henriksen, A., Hansen, F. G., and Winther, J. R. (2001) Shedding light on disulfide bond formation: Engineering a redox switch in green fluorescent protein. *EMBO J. 20*, 5853−5862.

(16) Millet, O., Hudson, R. P., and Kay, L. E. (2003) The energetic cost of domain reorientation in maltose-binding protein as studied by NMR and fluorescence spectroscopy. *Proc. Natl. Acad. Sci. U.S.A. 100*, 12700−12705.

(17) Ke, W., Laurent, A. H., Armstrong, M. D., Chen, Y., Smith, W. E., Liang, J., Wright, C. M., Ostermeier, M., and van den Akker, F. (2012) Structure of an engineered β-lactamase maltose binding protein fusion protein: Insights into heterotropic allosteric regulation. *PLoS One 7*, e39168.

(18) Krivov, G. G., Shapovalov, M. V., and Dunbrack, R. L., Jr. (2009) Improved prediction of protein side-chain conformations with SCWRL4. *Proteins 77*, 778−795.

(19) Liang, J., Kim, J. R., Boock, J. T., Mansell, T. J., and Ostermeier, M. (2007) Ligand binding and allostery can emerge simultaneously. *Protein Sci. 16*, 929−937.

(20) Heins, R. A., Choi, J. H., Sohka, T., and Ostermeier, M. (2011) *In vitro* recombination of non-homologous genes can result in gene fusions that confer a switching phenotype to cells. *PLoS One 6*, e27302.

(21) Choi, J. H., San, A., and Ostermeier, M. (2013) Non-allosteric enzyme switches possess larger effector-induced changes in thermodynamic stability than their non-switch analogs. *Protein Sci. 22*, 475−485.

(22) Telmer, P. G., and Shilton, B. H. (2003) Insights into the conformational equilibria of maltose-binding protein by analysis of high affinity mutants. *J. Biol. Chem. 278*, 34555−34567.

(23) Sohka, T., Heins, R. A., Phelan, R. M., Greisler, J. M., Townsend, C. A., and Ostermeier, M. (2009) An externally tunable bacterial band-pass filter. *Proc. Natl. Acad. Sci. U.S.A. 106*, 10135−10140.

(24) Wright, C. M., Wright, R. C., Eshleman, J. R., and Ostermeier, M. (2011) A protein therapeutic modality founded on molecular regulation. *Proc. Natl. Acad. Sci. U.S.A. 108*, 16206−16211.

(25) Van Der Spoel, D., Lindahl, E., Hess, B., Groenhof, G., Mark, A. E., and Berendsen, H. J. (2005) GROMACS: Fast, flexible, and free. *J. Comput. Chem. 26*, 1701−1718.

(26) Pettersen, E. F., Goddard, T. D., Huang, C. C., Couch, G. S., Greenblatt, D. M., Meng, E. C., and Ferrin, T. E. (2004) UCSF Chimera—A visualization system for exploratory research and analysis. *J. Comput. Chem. 25*, 1605−1612.